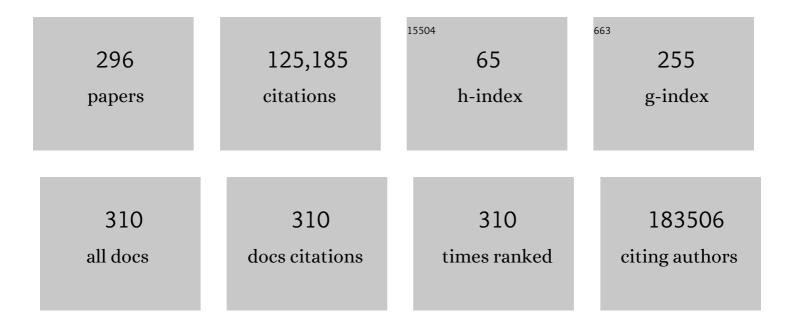
List of Publications by Year in descending order

Source: https://exaly.com/author-pdf/1762642/publications.pdf Version: 2024-02-01



#	Article	IF	CITATIONS
1	Fiji: an open-source platform for biological-image analysis. Nature Methods, 2012, 9, 676-682.	19.0	47,818
2	NIH Image to ImageJ: 25 years of image analysis. Nature Methods, 2012, 9, 671-675.	19.0	46,756
3	ImageJ2: ImageJ for the next generation of scientific image data. BMC Bioinformatics, 2017, 18, 529.	2.6	4,464
4	TrackMate: An open and extensible platform for single-particle tracking. Methods, 2017, 115, 80-90.	3.8	2,546
5	The ImageJ ecosystem: An open platform for biomedical image analysis. Molecular Reproduction and Development, 2015, 82, 518-529.	2.0	2,029
6	Trainable Weka Segmentation: a machine learning tool for microscopy pixel classification. Bioinformatics, 2017, 33, 2424-2426.	4.1	1,505
7	Collagen reorganization at the tumor-stromal interface facilitates local invasion. BMC Medicine, 2006, 4, 38.	5.5	1,417
8	Collagen density promotes mammary tumor initiation and progression. BMC Medicine, 2008, 6, 11.	5.5	1,129
9	Aligned Collagen Is a Prognostic Signature for Survival in Human Breast Carcinoma. American Journal of Pathology, 2011, 178, 1221-1232.	3.8	1,026
10	Improved structure, function and compatibility for CellProfiler: modular high-throughput image analysis software. Bioinformatics, 2011, 27, 1179-1180.	4.1	948
11	<i>In vivo</i> multiphoton microscopy of NADH and FAD redox states, fluorescence lifetimes, and cellular morphology in precancerous epithelia. Proceedings of the National Academy of Sciences of the United States of America, 2007, 104, 19494-19499.	7.1	898
12	Metadata matters: access to image data in the real world. Journal of Cell Biology, 2010, 189, 777-782.	5.2	858
13	Matrix density-induced mechanoregulation of breast cell phenotype, signaling and gene expression through a FAK–ERK linkage. Oncogene, 2009, 28, 4326-4343.	5.9	557
14	Biological imaging software tools. Nature Methods, 2012, 9, 697-710.	19.0	462
15	Contact Guidance Mediated Three-Dimensional Cell Migration is Regulated by Rho/ROCK-Dependent Matrix Reorganization. Biophysical Journal, 2008, 95, 5374-5384.	0.5	426
16	Beyond the margins: real-time detection of cancer using targeted fluorophores. Nature Reviews Clinical Oncology, 2017, 14, 347-364.	27.6	366
17	Metabolic Mapping of MCF10A Human Breast Cells via Multiphoton Fluorescence Lifetime Imaging of the Coenzyme NADH. Cancer Research, 2005, 65, 8766-8773.	0.9	351
18	3D Collagen Alignment Limits Protrusions to Enhance Breast Cancer Cell Persistence. Biophysical Journal, 2014, 107, 2546-2558.	0.5	346

#	Article	IF	CITATIONS
19	Postpartum mammary gland involution drives progression of ductal carcinoma in situ through collagen and COX-2. Nature Medicine, 2011, 17, 1109-1115.	30.7	318
20	In vivo multiphoton fluorescence lifetime imaging of protein-bound and free nicotinamide adenine dinucleotide in normal and precancerous epithelia. Journal of Biomedical Optics, 2007, 12, 024014.	2.6	317
21	OpenSPIM: an open-access light-sheet microscopy platform. Nature Methods, 2013, 10, 598-599.	19.0	312
22	The collagen receptor discoidin domain receptor 2 stabilizes SNAIL1 to facilitate breast cancer metastasis. Nature Cell Biology, 2013, 15, 677-687.	10.3	312
23	Computational segmentation of collagen fibers from second-harmonic generation images of breast cancer. Journal of Biomedical Optics, 2014, 19, 016007.	2.6	294
24	Dual-stream Multiple Instance Learning Network for Whole Slide Image Classification with Self-supervised Contrastive Learning. , 2021, 2021, 14318-14328.		216
25	Multiphoton Microscopy of Endogenous Fluorescence Differentiates Normal, Precancerous, and Cancerous Squamous Epithelial Tissues. Cancer Research, 2005, 65, 1180-1186.	0.9	214
26	Transition to invasion in breast cancer: a microfluidic in vitro model enables examination of spatial and temporal effects. Integrative Biology (United Kingdom), 2011, 3, 439-450.	1.3	201
27	Non-line-of-sight imaging using a time-gated single photon avalanche diode. Optics Express, 2015, 23, 20997.	3.4	194
28	Multiphoton microscopy and fluorescence lifetime imaging microscopy (FLIM) to monitor metastasis and the tumor microenvironment. Clinical and Experimental Metastasis, 2009, 26, 357-370.	3.3	185
29	Automated quantification of aligned collagen for human breast carcinoma prognosis. Journal of Pathology Informatics, 2014, 5, 28.	1.7	172
30	Lineage Reprogramming of Fibroblasts into Proliferative Induced Cardiac Progenitor Cells by Defined Factors. Cell Stem Cell, 2016, 18, 354-367.	11.1	165
31	Highly aligned stromal collagen is a negative prognostic factor following pancreatic ductal adenocarcinoma resection. Oncotarget, 2016, 7, 76197-76213.	1.8	163
32	Anthocyanin Vacuolar Inclusions Form by a Microautophagy Mechanism. Plant Cell, 2015, 27, 2545-2559.	6.6	153
33	A subset of myofibroblastic cancer-associated fibroblasts regulate collagen fiber elongation, which is prognostic in multiple cancers. Oncotarget, 2016, 7, 6159-6174.	1.8	149
34	Control of 3-dimensional collagen matrix polymerization for reproducible human mammary fibroblast cell culture in microfluidic devices. Biomaterials, 2009, 30, 4833-4841.	11.4	138
35	Neuroendocrine Tumorâ€Targeted Upconversion Nanoparticleâ€Based Micelles for Simultaneous NIRâ€Controlled Combination Chemotherapy and Photodynamic Therapy, and Fluorescence Imaging. Advanced Functional Materials, 2017, 27, 1604671.	14.9	138
36	Mammary Epithelial-Specific Disruption of Focal Adhesion Kinase Retards Tumor Formation and Metastasis in a Transgenic Mouse Model of Human Breast Cancer. American Journal of Pathology, 2008, 173, 1551-1565.	3.8	126

#	Article	IF	CITATIONS
37	Fluorescence Lifetime Imaging of Endogenous Fluorophores in Histopathology Sections Reveals Differences Between Normal and Tumor Epithelium in Carcinoma In Situ of the Breast. Cell Biochemistry and Biophysics, 2009, 53, 145-157.	1.8	125
38	Integrated studies of biology: multiplexed imaging assays from molecules to man and back. Current Opinion in Biotechnology, 2009, 20, 1-3.	6.6	119
39	A call for bioimaging software usability. Nature Methods, 2012, 9, 666-670.	19.0	116
40	Methods for Quantifying Fibrillar Collagen Alignment. Methods in Molecular Biology, 2017, 1627, 429-451.	0.9	115
41	Stiff Collagen Matrices Increase Tumorigenic Prolactin Signaling in Breast Cancer Cells. Journal of Biological Chemistry, 2013, 288, 12722-12732.	3.4	112
42	Matrix metalloproteinase 9 modulates collagen matrices and wound repair. Development (Cambridge), 2015, 142, 2136-2146.	2.5	111
43	Periductal stromal collagen topology of pancreatic ductal adenocarcinoma differs from that of normal and chronic pancreatitis. Modern Pathology, 2015, 28, 1470-1480.	5.5	110
44	Quantitating the cell: turning images into numbers with <scp>ImageJ</scp> . Wiley Interdisciplinary Reviews: Developmental Biology, 2017, 6, e260.	5.9	108
45	CGEF-1 and CHIN-1 Regulate CDC-42 Activity during Asymmetric Division in the <i>Caenorhabditis elegans</i> Embryo. Molecular Biology of the Cell, 2010, 21, 266-277.	2.1	105
46	Elevated collagen-I augments tumor progressive signals, intravasation and metastasis of prolactin-induced estrogen receptor alpha positive mammary tumor cells. Breast Cancer Research, 2017, 19, 9.	5.0	104
47	Filamin A–β1 Integrin Complex Tunes Epithelial Cell Response to Matrix Tension. Molecular Biology of the Cell, 2009, 20, 3224-3238.	2.1	103
48	The <scp>ImageJ</scp> ecosystem: Openâ€source software for image visualization, processing, and analysis. Protein Science, 2021, 30, 234-249.	7.6	102
49	Simultaneous two-photon spectral and lifetime fluorescence microscopy. Applied Optics, 2004, 43, 5173.	2.1	98
50	Cortical granule exocytosis in <i>C. elegans</i> is regulated by cell cycle components including separase. Development (Cambridge), 2007, 134, 3837-3848.	2.5	98
51	Bioimage Informatics for Experimental Biology. Annual Review of Biophysics, 2009, 38, 327-346.	10.0	98
52	Multi-functional self-fluorescent unimolecular micelles for tumor-targeted drug delivery and bioimaging. Biomaterials, 2015, 47, 41-50.	11.4	96
53	Tumor mechanics and metabolic dysfunction. Free Radical Biology and Medicine, 2015, 79, 269-280.	2.9	95
54	Aging and caloric restriction impact adipose tissue, adiponectin, and circulating lipids. Aging Cell, 2017, 16, 497-507.	6.7	94

#	Article	IF	CITATIONS
55	Collagen Alignment as a Predictor of Recurrence after Ductal Carcinoma <i>In Situ</i> . Cancer Epidemiology Biomarkers and Prevention, 2018, 27, 138-145.	2.5	94
56	Membrane dynamics during cellular wound repair. Molecular Biology of the Cell, 2016, 27, 2272-2285.	2.1	87
57	Induction of fibroblast senescence generates a non-fibrogenic myofibroblast phenotype that differentially impacts on cancer prognosis. Aging, 2016, 9, 114-132.	3.1	86
58	The Action of Discoidin Domain Receptor 2 in Basal Tumor Cells and Stromal Cancer-Associated Fibroblasts Is Critical for Breast Cancer Metastasis. Cell Reports, 2016, 15, 2510-2523.	6.4	85
59	Complex and Noncentrosymmetric Stacking of Layered Metal Dichalcogenide Materials Created by Screw Dislocations. Journal of the American Chemical Society, 2017, 139, 3496-3504.	13.7	81
60	Structural changes in mixed Col I/Col V collagen gels probed by SHG microscopy: implications for probing stromal alterations in human breast cancer. Biomedical Optics Express, 2011, 2, 2307.	2.9	78
61	Microtubules regulate GEF-H1 in response to extracellular matrix stiffness. Molecular Biology of the Cell, 2012, 23, 2583-2592.	2.1	78
62	Association of collagen architecture with glioblastoma patient survival. Journal of Neurosurgery, 2016, 126, 1812-1821.	1.6	78
63	Selected mitochondrial DNA landscapes activate the SIRT3 axis of the UPRmt to promote metastasis. Oncogene, 2017, 36, 4393-4404.	5.9	78
64	Fluorescence of Picrosirius Red Multiplexed With Immunohistochemistry for the Quantitative Assessment of Collagen in Tissue Sections. Journal of Histochemistry and Cytochemistry, 2017, 65, 479-490.	2.5	78
65	The Presence of Cyclooxygenase 2, Tumor-Associated Macrophages, and Collagen Alignment as Prognostic Markers for Invasive Breast Carcinoma Patients. American Journal of Pathology, 2018, 188, 559-573.	3.8	75
66	Harnessing non-destructive 3D pathology. Nature Biomedical Engineering, 2021, 5, 203-218.	22.5	74
67	Second-harmonic generation imaging of cancer. Methods in Cell Biology, 2014, 123, 531-546.	1.1	73
68	Distinct inflammatory and wound healing responses to complex caudal fin injuries of larval zebrafish. ELife, 2019, 8, .	6.0	72
69	Characterization of Fibrillar Collagens and Extracellular Matrix of Glandular Benign Prostatic Hyperplasia Nodules. PLoS ONE, 2014, 9, e109102.	2.5	71
70	Cortex-wide neural interfacing via transparent polymer skulls. Nature Communications, 2019, 10, 1500.	12.8	71
71	Comparison of Picrosirius Red Staining With Second Harmonic Generation Imaging for the Quantification of Clinically Relevant Collagen Fiber Features in Histopathology Samples. Journal of Histochemistry and Cytochemistry, 2016, 64, 519-529.	2.5	68
72	A shift in energy metabolism anticipates the onset of sarcopenia in rhesus monkeys. Aging Cell, 2013, 12, 672-681.	6.7	66

#	Article	IF	CITATIONS
73	Spatial and Temporal Analysis of Extracellular Matrix Proteins in the Developing Murine Heart: A Blueprint for Regeneration. Tissue Engineering - Part A, 2013, 19, 1132-1143.	3.1	65
74	In Vivo Visualization of Stromal Macrophages via label-free FLIM-based metabolite imaging. Scientific Reports, 2016, 6, 25086.	3.3	65
75	A Three-Dimensional Computational Model of Collagen Network Mechanics. PLoS ONE, 2014, 9, e111896.	2.5	63
76	The effect of micro-ECoG substrate footprint on the meningeal tissue response. Journal of Neural Engineering, 2014, 11, 046011.	3.5	63
77	Pancreatic β-Cells From Mice Offset Age-Associated Mitochondrial Deficiency With Reduced KATP Channel Activity. Diabetes, 2016, 65, 2700-2710.	0.6	59
78	Laser Scanning Confocal Microscopy: History, Applications, and Related Optical Sectioning Techniques. Methods in Molecular Biology, 2014, 1075, 9-47.	0.9	58
79	Extraction of optical properties and prediction of light distribution in rat brain tissue. Journal of Biomedical Optics, 2014, 19, 075001.	2.6	57
80	Mechanical signals regulate and activate SNAIL1 protein to control the fibrogenic response of CAFs. Journal of Cell Science, 2016, 129, 1989-2002.	2.0	57
81	Damage-induced reactive oxygen species regulate vimentin and dynamic collagen-based projections to mediate wound repair. ELife, 2018, 7, .	6.0	57
82	Nonlinear Optical Imaging of Cellular Processes in Breast Cancer. Microscopy and Microanalysis, 2008, 14, 532-548.	0.4	56
83	Shining new light on 3D cell motility and the metastatic process. Trends in Cell Biology, 2009, 19, 638-648.	7.9	56
84	GSK3β Regulates Brain Energy Metabolism. Cell Reports, 2018, 23, 1922-1931.e4.	6.4	55
85	Nonlinear optical microscopy and ultrasound imaging of human cervical structure. Journal of Biomedical Optics, 2013, 18, 031110.	2.6	54
86	Calsyntenin-1 Regulates Axon Branching and Endosomal Trafficking during Sensory Neuron Development In Vivo. Journal of Neuroscience, 2014, 34, 9235-9248.	3.6	54
87	OptogenSIM: a 3D Monte Carlo simulation platform for light delivery design in optogenetics. Biomedical Optics Express, 2015, 6, 4859.	2.9	54
88	Pycro-Manager: open-source software for customized and reproducible microscope control. Nature Methods, 2021, 18, 226-228.	19.0	54
89	Optical workstation with concurrent, independent multiphoton imaging and experimental laser microbeam capabilities. Review of Scientific Instruments, 2003, 74, 193-201.	1.3	54
90	SORCS1 is necessary for normal insulin secretory granule biogenesis in metabolically stressed β cells. Journal of Clinical Investigation, 2014, 124, 4240-4256.	8.2	53

#	Article	IF	CITATIONS
91	Nonlinear optical imaging and spectral-lifetime computational analysis of endogenous and exogenous fluorophores in breast cancer. Journal of Biomedical Optics, 2008, 13, 031220.	2.6	52
92	A bioengineered heterotypic stroma–cancer microenvironment model to study pancreatic ductal adenocarcinoma. Lab on A Chip, 2013, 13, 3965.	6.0	51
93	3D texture analysis for classification of second harmonic generation images of human ovarian cancer. Scientific Reports, 2016, 6, 35734.	3.3	51
94	Targeted matrisome analysis identifies thrombospondin-2 and tenascin-C in aligned collagen stroma from invasive breast carcinoma. Scientific Reports, 2018, 8, 12941.	3.3	51
95	Calcific Aortic Valve Disease Is Associated with Layer-Specific Alterations in Collagen Architecture. PLoS ONE, 2016, 11, e0163858.	2.5	50
96	Open-source deep-learning software for bioimage segmentation. Molecular Biology of the Cell, 2021, 32, 823-829.	2.1	50
97	Dense Collagen-I Matrices Enhance Pro-Tumorigenic Estrogen-Prolactin Crosstalk in MCF-7 and T47D Breast Cancer Cells. PLoS ONE, 2015, 10, e0116891.	2.5	48
98	Open source bioimage informatics for cell biology. Trends in Cell Biology, 2009, 19, 656-660.	7.9	47
99	Closed-Loop Optogenetic Brain Interface. IEEE Transactions on Biomedical Engineering, 2015, 62, 2327-2337.	4.2	46
100	Autofluorescence lifetime imaging of cellular metabolism: Sensitivity toward cell density, pH, intracellular, and intercellular heterogeneity. Cytometry Part A: the Journal of the International Society for Analytical Cytology, 2019, 95, 56-69.	1.5	46
101	Charcot-Marie-Tooth 2b associated Rab7 mutations cause axon growth and guidance defects during vertebrate sensory neuron development. Neural Development, 2016, 11, 2.	2.4	43
102	Analysis of histology specimens using lifetime multiphoton microscopy. Journal of Biomedical Optics, 2003, 8, 376.	2.6	42
103	Navigating the Collagen Jungle: The Biomedical Potential of Fiber Organization in Cancer. Bioengineering, 2021, 8, 17.	3.5	42
104	Lactation opposes pappalysinâ€1â€driven pregnancyâ€associated breast cancer. EMBO Molecular Medicine, 2016, 8, 388-406.	6.9	41
105	Enriching Islet Phospholipids With Eicosapentaenoic Acid Reduces Prostaglandin E2 Signaling and Enhances Diabetic Î ² -Cell Function. Diabetes, 2017, 66, 1572-1585.	0.6	41
106	Collagen organization of renal cell carcinoma differs between low and high grade tumors. BMC Cancer, 2019, 19, 490.	2.6	41
107	Visualization approaches for multidimensional biological image data. BioTechniques, 2007, 43, S31-S36.	1.8	40
108	Administration of Non-Torsadogenic human Ether-Ã-go-go-Related Gene Inhibitors Is Associated with Better Survival for High hERG–Expressing Glioblastoma Patients. Clinical Cancer Research, 2017, 23, 73-80.	7.0	40

#	Article	IF	CITATIONS
109	Unifying biological image formats with HDF5. Communications of the ACM, 2009, 52, 42-47.	4.5	39
110	Quantification of Collagen Organization and Extracellular Matrix Factors within the Healing Ligament. Microscopy and Microanalysis, 2011, 17, 779-787.	0.4	39
111	Goniometric measurements of thick tissue using Monte Carlo simulations to obtain the single scattering anisotropy coefficient. Biomedical Optics Express, 2012, 3, 2707.	2.9	39
112	<scp>SHARPIN</scp> regulates collagen architecture and ductal outgrowth in the developing mouse mammary gland. EMBO Journal, 2017, 36, 165-182.	7.8	39
113	Quantification of collagen organization in histopathology samples using liquid crystal based polarization microscopy. Biomedical Optics Express, 2017, 8, 4243.	2.9	39
114	Resveratrol Metabolites Do Not Elicit Early Pro-apoptotic Mechanisms in Neuroblastoma Cells. Journal of Agricultural and Food Chemistry, 2011, 59, 4979-4986.	5.2	37
115	Void spot assay procedural optimization and software for rapid and objective quantification of rodent voiding function, including overlapping urine spots. American Journal of Physiology - Renal Physiology, 2018, 315, F1067-F1080.	2.7	37
116	Blue Light Modulates Murine Microglial Gene Expression in the Absence of Optogenetic Protein Expression. Scientific Reports, 2016, 6, 21172.	3.3	36
117	Mesenchymal Stem Cell Interactions with 3D ECM Modules Fabricated via Multiphoton Excited Photochemistry. Biomacromolecules, 2012, 13, 2917-2925.	5.4	35
118	ImageJ-MATLAB: a bidirectional framework for scientific image analysis interoperability. Bioinformatics, 2017, 33, 629-630.	4.1	35
119	Syndecan-1 induction in lung microenvironment supports the establishment of breast tumor metastases. Breast Cancer Research, 2018, 20, 66.	5.0	35
120	VisBio: A Computational Tool for Visualization of Multidimensional Biological Image Data. Traffic, 2004, 5, 411-417.	2.7	33
121	Tools for Visualizing Multidimensional Images from Living Specimens. Photochemistry and Photobiology, 2005, 81, 1116.	2.5	33
122	Lrrc10 is required for early heart development and function in zebrafish. Developmental Biology, 2007, 308, 494-506.	2.0	33
123	Human pancreatic stellate cells modulate 3D collagen alignment to promote the migration of pancreatic ductal adenocarcinoma cells. Biomedical Microdevices, 2016, 18, 105.	2.8	33
124	Chemically Derived Kirigami of WSe ₂ . Journal of the American Chemical Society, 2018, 140, 10980-10987.	13.7	33
125	Applications of combined spectral lifetime microscopy for biology. BioTechniques, 2006, 41, 249-257.	1.8	32
126	Fibrillar Collagen Quantification With Curvelet Transform Based Computational Methods. Frontiers in Bioengineering and Biotechnology, 2020, 8, 198.	4.1	32

#	Article	IF	CITATIONS
127	A microfluidic coculture and multiphoton FAD analysis assay provides insight into the influence of the bone microenvironment on prostate cancer cells. Integrative Biology (United Kingdom), 2014, 6, 627-635.	1.3	31
128	zWEDGI: Wounding and Entrapment Device for Imaging Live Zebrafish Larvae. Zebrafish, 2017, 14, 42-50.	1.1	31
129	The Kinesin Adaptor Calsyntenin-1 Organizes Microtubule Polarity and Regulates Dynamics during Sensory Axon Arbor Development. Frontiers in Cellular Neuroscience, 2017, 11, 107.	3.7	31
130	Molecular and Functional Networks Linked to Sarcopenia Prevention by Caloric Restriction in Rhesus Monkeys. Cell Systems, 2020, 10, 156-168.e5.	6.2	31
131	ECM-Incorporated Hydrogels Cross-Linked via Native Chemical Ligation To Engineer Stem Cell Microenvironments. Biomacromolecules, 2013, 14, 3102-3111.	5.4	30
132	Quantitative Histopathology of Stained Tissues using Color Spatial Light Interference Microscopy (cSLIM). Scientific Reports, 2019, 9, 14679.	3.3	30
133	Applying Multiphoton Imaging to the Study of Membrane Dynamics in Living Cells. Traffic, 2001, 2, 775-780.	2.7	29
134	Engineering Threeâ€Dimensional Collagen Matrices to Provide Contact Guidance during 3D Cell Migration. Current Protocols in Cell Biology, 2010, 47, Unit 10.17.	2.3	29
135	A nondenatured, noncrosslinked collagen matrix to deliver stem cells to the heart. Regenerative Medicine, 2011, 6, 569-582.	1.7	29
136	Experimental and simulation study of the wavelength dependent second harmonic generation of collagen in scattering tissues. Optics Letters, 2014, 39, 1897.	3.3	29
137	Image-inspired 3D multiphoton excited fabrication of extracellular matrix structures by modulated raster scanning. Optics Express, 2013, 21, 25346.	3.4	28
138	RhoA is down-regulated at cell–cell contacts via p190RhoGAP-B in response to tensional homeostasis. Molecular Biology of the Cell, 2013, 24, 1688-1699.	2.1	27
139	Regional metabolic heterogeneity of the hippocampus is nonuniformly impacted by age and caloric restriction. Aging Cell, 2016, 15, 100-110.	6.7	27
140	Stromal alterations in ovarian cancers via wavelength dependent Second Harmonic Generation microscopy and optical scattering. BMC Cancer, 2017, 17, 102.	2.6	27
141	Scientific Community Image Forum: A discussion forum for scientific image software. PLoS Biology, 2019, 17, e3000340.	5.6	27
142	Imaging cardiac extracellular matrices: a blueprint for regeneration. Trends in Biotechnology, 2012, 30, 233-240.	9.3	25
143	SCIFIO: an extensible framework to support scientific image formats. BMC Bioinformatics, 2016, 17, 521.	2.6	25
144	PGCâ€la integrates a metabolism and growth network linked to caloric restriction. Aging Cell, 2019, 18, e12999.	6.7	25

9

#	Article	IF	CITATIONS
145	Single image super-resolution for whole slide image using convolutional neural networks and self-supervised color normalization. Medical Image Analysis, 2021, 68, 101938.	11.6	25
146	Machine Learning Methods for Fluorescence Lifetime Imaging (FLIM) Based Label-Free Detection of Microglia. Frontiers in Neuroscience, 2020, 14, 931.	2.8	24
147	Integration of the ImageJ Ecosystem in KNIME Analytics Platform. Frontiers in Computer Science, 2020, 2, .	2.8	24
148	Drosophila TRIM32 cooperates with glycolytic enzymes to promote cell growth. ELife, 2020, 9, .	6.0	24
149	Cooperativity among Rev-Associated Nuclear Export Signals Regulates HIV-1 Gene Expression and Is a Determinant of Virus Species Tropism. Journal of Virology, 2014, 88, 14207-14221.	3.4	23
150	Non-disruptive collagen characterization in clinical histopathology using cross-modality image synthesis. Communications Biology, 2020, 3, 414.	4.4	23
151	FLIMJ: An open-source ImageJ toolkit for fluorescence lifetime image data analysis. PLoS ONE, 2020, 15, e0238327.	2.5	23
152	Validation of an arterial constitutive model accounting for collagen content and crosslinking. Acta Biomaterialia, 2016, 31, 276-287.	8.3	22
153	NAD(P)H fluorescence lifetime measurements in fixed biological tissues. Methods and Applications in Fluorescence, 2019, 7, 044005.	2.3	22
154	Quantitative phase imaging of stromal prognostic markers in pancreatic ductal adenocarcinoma. Biomedical Optics Express, 2020, 11, 1354.	2.9	22
155	Cell death, nonâ€invasively assessed by intrinsic fluorescence intensity of NADH, is a predictive indicator of functional differentiation of embryonic stem cells. Biology of the Cell, 2012, 104, 352-364.	2.0	21
156	Advanced materials for neural surface electrodes. Current Opinion in Solid State and Materials Science, 2014, 18, 301-307.	11.5	21
157	ImageJ for the Next Generation of Scientific Image Data. Microscopy and Microanalysis, 2019, 25, 142-143.	0.4	21
158	Collagen Organization in Relation to Ductal Carcinoma <i>In Situ</i> Pathology and Outcomes. Cancer Epidemiology Biomarkers and Prevention, 2021, 30, 80-88.	2.5	21
159	Developing open-source software for bioimage analysis: opportunities and challenges. F1000Research, 2021, 10, 302.	1.6	20
160	ImageJ and CellProfiler: Complements in Openâ€Source Bioimage Analysis. Current Protocols, 2021, 1, e89.	2.9	20
161	Prolactin signaling through focal adhesion complexes is amplified by stiff extracellular matrices in breast cancer cells. Oncotarget, 2016, 7, 48093-48106.	1.8	20
162	Three-dimensional surface profiling and optical characterization of liquid microlens using a Shack–Hartmann wave front sensor. Applied Physics Letters, 2011, 98, 171104.	3.3	19

#	Article	IF	CITATIONS
163	Association of cellular and molecular responses in the rat mammary gland to 17β-estradiol with susceptibility to mammary cancer. BMC Cancer, 2013, 13, 573.	2.6	19
164	Using fluorescence lifetime microscopy to study the subcellular localization of anthocyanins. Plant Journal, 2016, 88, 895-903.	5.7	19
165	Optimization of interstrand interactions enables burn detection with a collagen-mimetic peptide. Organic and Biomolecular Chemistry, 2019, 17, 9906-9912.	2.8	19
166	Nonparametric empirical Bayesian framework for fluorescence-lifetime imaging microscopy. Biomedical Optics Express, 2019, 10, 5497.	2.9	19
167	Intensity-based registration of bright-field and second-harmonic generation images of histopathology tissue sections. Biomedical Optics Express, 2020, 11, 160.	2.9	19
168	Multiphoton Flow Cytometry to Assess Intrinsic and Extrinsic Fluorescence in Cellular Aggregates: Applications to Stem Cells. Microscopy and Microanalysis, 2011, 17, 540-554.	0.4	18
169	Simultaneous determination of the second-harmonic generation emission directionality and reduced scattering coefficient from three-dimensional imaging of thick tissues. Journal of Biomedical Optics, 2013, 18, 116008.	2.6	18
170	Opportunities for multiple-beam synchrotron-based mid-infrared imaging at IRENI. Vibrational Spectroscopy, 2012, 60, 10-15.	2.2	17
171	Endogenous Fluorescence Signatures in Living Pluripotent Stem Cells Change with Loss of Potency. PLoS ONE, 2012, 7, e43708.	2.5	17
172	Mammary collagen architecture and its association with mammographic density and lesion severity among women undergoing image-guided breast biopsy. Breast Cancer Research, 2021, 23, 105.	5.0	17
173	3D second harmonic generation imaging tomography by multi-view excitation. Optica, 2017, 4, 1171.	9.3	16
174	Patterned Optogenetic Modulation of Neurovascular and Metabolic Signals. Journal of Cerebral Blood Flow and Metabolism, 2015, 35, 140-147.	4.3	15
175	Optical imaging of collagen fiber damage to assess thermally injured human skin. Wound Repair and Regeneration, 2020, 28, 848-855.	3.0	15
176	2020 BioImage Analysis Survey: Community experiences and needs for the future. Biological Imaging, 2022, 1, .	2.2	15
177	Three-Dimensional Surface Profile Measurement of Microlenses Using the Shack–Hartmann Wavefront Sensor. Journal of Microelectromechanical Systems, 2012, 21, 530-540.	2.5	14
178	Second Harmonic Generation Imaging of Collagen in Chronically Implantable Electrodes in Brain Tissue. Frontiers in Neuroscience, 2020, 14, 95.	2.8	14
179	Review of quantitative multiscale imaging of breast cancer. Journal of Medical Imaging, 2018, 5, 1.	1.5	14
180	Endogenous Optical Signals Reveal Changes of Elastin and Collagen Organization During Differentiation of Mouse Embryonic Stem Cells. Tissue Engineering - Part C: Methods, 2015, 21, 995-1004.	2.1	13

#	ARTICLE	IF	CITATIONS
181	A beam optics study of a modular multi-source X-ray tube for novel computed tomography applications. Nuclear Instruments and Methods in Physics Research, Section A: Accelerators, Spectrometers, Detectors and Associated Equipment, 2017, 868, 1-9.	1.6	13
182	Convolutional neural networks for whole slide image superresolution. Biomedical Optics Express, 2018, 9, 5368.	2.9	13
183	Distinct Tissue Damage and Microbial Cues Drive Neutrophil and Macrophage Recruitment to Thermal Injury. IScience, 2020, 23, 101699.	4.1	13
184	Nonlinear optical microscopy and computational analysis of intrinsic signatures in breast cancer. , 2009, 2009, 4077-80.		12
185	The ImageJ Ecosystem: An Open and Extensible Platform for Biomedical Image Analysis Microscopy and Microanalysis, 2017, 23, 226-227.	0.4	12
186	Imaging the Cardiac Extracellular Matrix. Advances in Experimental Medicine and Biology, 2018, 1098, 21-44.	1.6	12
187	Changes in Cutaneous Gene Expression after Microvascular Free Tissue Transfer in Parry-Romberg Syndrome. Plastic and Reconstructive Surgery, 2018, 142, 303e-309e.	1.4	12
188	Transglutaminase-2 Mediates the Biomechanical Properties of the Colorectal Cancer Tissue Microenvironment that Contribute to Disease Progression. Cancers, 2019, 11, 701.	3.7	12
189	A novel bioreactor for combined magnetic resonance spectroscopy and optical imaging of metabolism in 3D cell cultures. Magnetic Resonance in Medicine, 2019, 81, 3379-3391.	3.0	12
190	Modeling early thermal injury using an ex vivo human skin model of contact burns. Burns, 2021, 47, 611-620.	1.9	12
191	Ellipsoid Zone Defects in Retinal Vein Occlusion Correlates With Visual Acuity Prognosis: SCORE2 Report 14. Translational Vision Science and Technology, 2021, 10, 31.	2.2	12
192	Real-time polarization microscopy of fibrillar collagen in histopathology. Scientific Reports, 2021, 11, 19063.	3.3	12
193	Super-resolution recurrent convolutional neural networks for learning with multi-resolution whole slide images. Journal of Biomedical Optics, 2019, 24, 1.	2.6	12
194	Automated and Robust Quantification of Colocalization in Dual-Color Fluorescence Microscopy: A Nonparametric Statistical Approach. IEEE Transactions on Image Processing, 2018, 27, 622-636.	9.8	11
195	Bimolecular fluorescence complementation analysis of eukaryotic fusion products. Biology of the Cell, 2010, 102, 525-537.	2.0	10
196	Preparation of 3D Collagen Gels and Microchannels for the Study of 3D Interactions In Vivo . Journal of Visualized Experiments, 2016, , .	0.3	10
197	Diverse activities of viralcis-acting RNA regulatory elements revealed using multicolor, long-term, single-cell imaging. Molecular Biology of the Cell, 2017, 28, 476-487.	2.1	10
198	Quantification of Collagen Organization after Nerve Repair. Plastic and Reconstructive Surgery - Global Open, 2017, 5, e1586.	0.6	10

#	Article	IF	CITATIONS
199	Spatially Adaptive Colocalization Analysis in Dual-Color Fluorescence Microscopy. IEEE Transactions on Image Processing, 2019, 28, 4471-4485.	9.8	10
200	Rhesus monkeys as a translational model for lateâ€onset Alzheimer's disease. Aging Cell, 2021, 20, e13374.	6.7	10
201	Student Learning of Early Embryonic Development via the Utilization of Research Resources from the Nematode <i>Caenorhabditis elegans</i> . CBE Life Sciences Education, 2008, 7, 64-73.	2.3	9
202	Expression of the <i>Drosophila</i> homeobox gene, <i>Distalâ€less</i> , supports an ancestral role in neural development. Developmental Dynamics, 2016, 245, 87-95.	1.8	9
203	A semi-automated machine-learning based workflow for ellipsoid zone analysis in eyes with macular edema: SCORE2 pilot study. PLoS ONE, 2020, 15, e0232494.	2.5	9
204	Microstructure and resident cell-types of the feline optic nerve head resemble that of humans. Experimental Eye Research, 2021, 202, 108315.	2.6	9
205	Citrullination regulates wound responses and tissue regeneration in zebrafish. Journal of Cell Biology, 2020, 219, .	5.2	9
206	Detecting cervical microstructure via ultrasound and optical microscopy. , 2010, , .		8
207	A multiscale Mueller polarimetry module for a stereo zoom microscope. Biomedical Engineering Letters, 2019, 9, 339-349.	4.1	8
208	Impact of tissue preservation on collagen fiber architecture. Biotechnic and Histochemistry, 2019, 94, 134-144.	1.3	8
209	Evolution of ischemia and neovascularization in a murine model of full thickness human wound healing. Wound Repair and Regeneration, 2020, 28, 812-822.	3.0	8
210	Hyperpolarized 13C Magnetic Resonance Spectroscopic Imaging of Pyruvate Metabolism in Murine Breast Cancer Models of Different Metastatic Potential. Metabolites, 2021, 11, 274.	2.9	8
211	Joint regression-classification deep learning framework for analyzing fluorescence lifetime images using NADH and FAD. Biomedical Optics Express, 2021, 12, 2703.	2.9	8
212	Metabolic mapping of glioblastoma stem cells reveals NADH fluxes associated with glioblastoma phenotype and survival. Journal of Biomedical Optics, 2020, 25, 1.	2.6	8
213	Microglia activation visualization via fluorescence lifetime imaging microscopy of intrinsically fluorescent metabolic cofactors. Neurophotonics, 2020, 7, 1.	3.3	8
214	WormClassroom.org: An Inquiry-rich Educational Web Portal for Research Resources of Caenorhabditis elegans. CBE Life Sciences Education, 2007, 6, 98-108.	2.3	7
215	FunImageJ: a Lisp framework for scientific image processing. Bioinformatics, 2018, 34, 899-900.	4.1	7
216	Quantifying Fibrillar Collagen Organization with Curvelet Transform-Based Tools. Journal of Visualized Experiments, 2020, , .	0.3	7

#	Article	IF	CITATIONS
217	Multi-view second-harmonic generation imaging of mouse tail tendon via reflective micro-prisms. Optics Letters, 2015, 40, 3201.	3.3	6
218	Long-term Live Imaging Device for Improved Experimental Manipulation of Zebrafish Larvae. Journal of Visualized Experiments, 2017, , .	0.3	6
219	Advanced quantitative imaging and biomechanical analyses of periosteal fibers in accelerated bone growth. Bone, 2016, 92, 201-213.	2.9	5
220	Radiation Promptly Alters Cancer Live Cell Metabolic Fluxes: An In Vitro Demonstration. Radiation Research, 2016, 185, 496.	1.5	5
221	Recovery and Regrowth After Nerve Repair: A Systematic Analysis of Four Repair Techniques. Journal of Surgical Research, 2020, 251, 311-320.	1.6	5
222	A device for the controlled cooling and freezing of excised plant specimens during magnetic resonance imaging. Plant Methods, 2021, 17, 41.	4.3	5
223	Advanced Intestinal Cancers often Maintain a Multi-Ancestral Architecture. PLoS ONE, 2016, 11, e0150170.	2.5	5
224	An open source, 3D printed preclinical MRI phantom for repeated measures of contrast agents and reference standards. Biomedical Physics and Engineering Express, 2018, 4, 027005.	1.2	4
225	Cultured cardiac fibroblasts and myofibroblasts express Sushi Containing Domain 2 and assemble a unique fibronectin rich matrix. Experimental Cell Research, 2021, 399, 112489.	2.6	4
226	Structured Correlation Detection with Application to Colocalization Analysis in Dual-Channel Fluorescence Microscopic Imaging. Statistica Sinica, 2021, 31, 333-360.	0.3	4
227	Parallel multiphoton excited fabrication of tissue engineering scaffolds using a diffractive optical element. Optics Express, 2020, 28, 2744.	3.4	4
228	Abstract A35: Aligned collagen is a prognostic signature for survival in human breast carcinoma. , 2013, , .		4
229	Wavelet Compression of Three-Dimensional Time-Lapse Biological Image Data. Microscopy and Microanalysis, 2005, 11, 9-17.	0.4	3
230	Fast localized wavefront correction using area-mapped phase-shift interferometry. Optics Letters, 2011, 36, 2892.	3.3	3
231	ImageJ: Image Analysis Interoperability for the Next Generation of Biological Image Data. Microscopy and Microanalysis, 2016, 22, 2066-2067.	0.4	3
232	Imaging Vacuolar Anthocyanins with Fluorescence Lifetime Microscopy (FLIM). Methods in Molecular Biology, 2018, 1789, 131-141.	0.9	3
233	A Novel Anisotropy Imaging Technique for NAD(P)H Autofluorescence. Microscopy and Microanalysis, 2019, 25, 1246-1247.	0.4	3
234	Coding Scheme Optimization for Fast Fluorescence Lifetime Imaging. ACM Transactions on Graphics, 2019, 38, 1-16.	7.2	3

#	Article	IF	CITATIONS
235	3-D-Printed Registration Phantom for Combined Ultrasound and Optical Imaging of Biological Tissues. Ultrasound in Medicine and Biology, 2020, 46, 1808-1814.	1.5	3
236	A syringe adapter for reduced muscular strain and fatigue. Applied Ergonomics, 2020, 85, 103061.	3.1	3
237	New Extensibility and Scripting Tools in the ImageJ Ecosystem. Current Protocols, 2021, 1, e204.	2.9	3
238	Platform for quantitative multiscale imaging of tissue composition. Biomedical Optics Express, 2020, 11, 1927.	2.9	3
239	Meeting in the Middle: Towards Successful Multidisciplinary Bioimage Analysis Collaboration. Frontiers in Bioinformatics, 2022, 2, .	2.1	3
240	A Model of Discovery: The Role of Imaging Established and Emerging Non-mammalian Models in Neuroscience. Frontiers in Molecular Neuroscience, 2022, 15, 867010.	2.9	3
241	Molecular Expressions: Exploring the World of Optics and Microscopy http:microscopy.fsu.edu. Biology of the Cell, 2004, 96, 403-405.	2.0	2
242	BioClips of symmetric and asymmetric cell division. Biology of the Cell, 2007, 99, 289-295.	2.0	2
243	Visualization of Morphological and Molecular Features Associated with Chronic Ischemia in Bioengineered Human Skin. Microscopy and Microanalysis, 2010, 16, 117-131.	0.4	2
244	Second-harmonic generation and fluorescence lifetime imaging microscopy through a rodent mammary imaging window. Proceedings of SPIE, 2012, , .	0.8	2
245	Shedding Light. , 2019, , .		2
246	Evaluating the effectiveness of a lower extremity venous phantom on developing ultrasound examination skills and confidence. Ultrasound, 2021, 29, 18-26.	0.7	2
247	Hyperdimensional Imaging Contrast Using an Optical Fiber. Sensors, 2021, 21, 1201.	3.8	2
248	Measuring the spatial distribution of multiply scattered light using a de-scanned image sensor for examining retinal structure contrast. Optics Express, 2021, 29, 552.	3.4	2
249	Optical fiber-based dispersion for spectral discrimination in fluorescence lifetime imaging systems. Journal of Biomedical Optics, 2019, 25, 1.	2.6	2
250	Abstract 3000: Hypoxic primary tumor stress microenvironments prime DTCs in lungs for dormancy. Cancer Research, 2015, 75, 3000-3000.	0.9	2
251	Fluorescence lifetime-based intrinsic metabolic signatures of microglia cell (Conference) Tj ETQq1 1 0.784314 r	gBT /Overl	ock_10 Tf 50
252	Registration of multiphoton optical images of cervical tissue to quantitative ultrasound data. , 2012, ,		1

#	Article	IF	CITATIONS
253	A chronic window imaging device for the investigation of in vivo peripheral nerves. , 2014, 2014, 1985-8.		1
254	Fabrication approaches for the creation of physical models from microscopy data. 3D Printing in Medicine, 2017, 3, 2.	3.1	1
255	Design of an Open-Source Binary Micromultileaf Collimator for a Small Animal Microradiotherapy System. Journal of Medical Devices, Transactions of the ASME, 2017, 11, .	0.7	1
256	Neighborhood regularized image superresolution for applications to microscopic imaging. , 2018, , .		1
257	An Investigation Into the Challenges of Using Metal Additive Manufacturing for the Production of Patient-Specific Aneurysm Clips. Journal of Medical Devices, Transactions of the ASME, 2019, 13, .	0.7	1
258	Mammographic Density: Intersection of Advocacy, Science, and Clinical Practice. Current Breast Cancer Reports, 2019, 11, 100-110.	1.0	1
259	Response to letter to the editor on "The use of human ex vivo models in burn research – Developments and perspectives― Burns, 2021, 47, 968-969.	1.9	1
260	Challenges of conducting quantitative ultrasound with a multimodal optical imaging system. Physics in Medicine and Biology, 2021, 66, 035008.	3.0	1
261	In vivo Multiphoton Fluorescence Lifetime Imaging of Free and Protein-bound NADH in Normal and Pre-cancerous Epithelia. , 2006, , .		1
262	Hyperspectral Multi-Point Confocal Microscope. , 2013, , .		1
263	Abstract B02: Matrix stiffness regulates local metabolism of breast carcinoma cells. , 2015, , .		1
264	Matrix metalloproteinase 9 modulates collagen matrices and wound repair. Journal of Cell Science, 2015, 128, e1.1-e1.1.	2.0	1
265	HIV RGB: Automated Single-Cell Analysis of HIV-1 Rev-Dependent RNA Nuclear Export and Translation Using Image Processing in KNIME. Viruses, 2022, 14, 903.	3.3	1
266	VisBio: a Flexible Open-Source Visualization Package for Multidimensional Image Data. Microscopy Today, 2006, 14, 6-11.	0.3	0
267	Image reconstruction of multiphoton microscopy data. , 2009, , 803-806.		0
268	338: Detection of cervical collagen with quantitative ultrasound. American Journal of Obstetrics and Gynecology, 2011, 204, S138.	1.3	0
269	Surface profiling and characterization of microlenses utilizing a Shack-Hartmann wavefront sensor. , 2011, , .		0
270	1069 MULTIPHOTON MICROSCOPIC CHARACTERIZATION OF RENAL CELL CARCINOMA. Journal of Urology, 2013, 189, .	0.4	0

#	Article	IF	CITATIONS
271	BI-24 * COLLAGEN PLAYS A ROLE IN GLIOBLASTOMA TUMOR INVASION AND PATIENT SURVIVAL. Neuro-Oncology, 2014, 16, v28-v28.	1.2	0
272	MP36-04 QUANTIFICATION OF RENAL CELL OPTICAL BIOMARKERS USING SECOND HARMONIC GENERATION IMAGING. Journal of Urology, 2014, 191, .	0.4	0
273	Development of a Bioinspired Stroma Model to Study the Role of Collagen Topology in Pancreatic Ductal Adenocarcinoma. Microscopy and Microanalysis, 2015, 21, 87-88.	0.4	0
274	NAD(P)H-FLIM and FRET Imaging of Pancreatic Islet Oscillations Reveals Novel Activators of Mitochondrial Respiratory Complex I in the Setting of Obesity. Biophysical Journal, 2016, 110, 486a-487a.	0.5	0
275	TUDCA Rescues Î ³ -Cell Metabolic Oscillations from ER Stress, Revealed By NAD(P)H-FLIM and FRET. Biophysical Journal, 2016, 110, 142a-143a.	0.5	0
276	Wavelength dependent SHG imaging and scattering probes of extracellular matrix (ECM) alterations in ovarian cancer (Conference Presentation). , 2017, , .		0
277	Thermal Conductivity Measurement of Granular UO ₂ (NO ₃) ₂ · 6H ₂ O. Nuclear Technology, 2017, 197, 191-200.	1.2	0
278	Quantitative second harmonic generation imaging of leporine, canine, and porcine vocal fold collagen. Laryngoscope, 2019, 129, 2549-2556.	2.0	0
279	Abstract 18: Augmentation of the Wisconsin "Blue-Blood―Chicken Thigh Model with Fluorescent Imaging Enhances the Assessment of Anastomotic Patency in Supermicrosurgical Training. Plastic and Reconstructive Surgery - Global Open, 2020, 8, 10-11.	0.6	0
280	Open source remote monitoring of research lasers. Optics and Laser Technology, 2021, 143, 107363.	4.6	0
281	Chapter 3. Screening Approaches for Stem Cells. , 2010, , 45-80.		0
282	Abstract 4749: Aligned collagen is a prognostic signature for survival in human breast carcinoma. , 2011, , .		0
283	Abstract 4960: COX-2 inhibition with celecoxib delays the progression of invasive mammary carcinoma in a murine model of collagen dense stroma , 2013, , .		0
284	Abstract 1116: Response to cyclooxygenase-2 inhibition is regulated by collagen dense stroma. , 2014, , .		0
285	Exposure to Optogenetic Blue Light Attenuates Inflammatory Gene Expression in Nonâ€transgenic Murine Microglia. FASEB Journal, 2015, 29, 835.5.	0.5	0
286	Abstract 332: Extracellular matrix stiffness regulates metabolic state in metastatic, but not quiescent, breast carcinoma cells. , 2015, , .		0
287	Abstract 4394: Phenotypic heterogeneity of disseminated tumor cells is predetermined by primary tumor hypoxic microenvironments. , 2016, , .		0
288	Sonification of hyperspectral fluorescence microscopy datasets. F1000Research, 0, 5, 2572.	1.6	0

#	Article	IF	CITATIONS
289	Abstract TMEM-015: QUANTITATIVE ASSESSMENT OF THE ROLE OF COLLAGEN ALTERATIONS IN OVARIAN CANCER. , 2017, , .		0
290	Abstract 3598: Classification of the collagen ECM in normal human tissue as a biomarker for future breast cancer incidence. , 2018, , .		0
291	Introduction to the Biophotonics Congress 2020 feature issue. Biomedical Optics Express, 2021, 12, 509.	2.9	0
292	Fluorescence Anisotropy in Autofluorescence Imaging and Metabolic Interpretations. , 2020, , .		0
293	FLIMJ: An open-source ImageJ toolkit for fluorescence lifetime image data analysis. , 2020, 15, e0238327.		0
294	FLIMJ: An open-source ImageJ toolkit for fluorescence lifetime image data analysis. , 2020, 15, e0238327.		0
295	FLIMJ: An open-source ImageJ toolkit for fluorescence lifetime image data analysis. , 2020, 15, e0238327.		0
296	FLIMJ: An open-source ImageJ toolkit for fluorescence lifetime image data analysis. , 2020, 15, e0238327.		0